ChemComm



FEATURE ARTICLE

View Article Online



Cite this: Chem. Commun., 2025, **61**. 4757

Received 27th November 2024, Accepted 19th February 2025

DOI: 10.1039/d4cc06307d

rsc.li/chemcomm

Recent development of azahelicenes showing circularly polarized luminescence

Chihiro Maeda ** and Tadashi Ema ***

Recently, a variety of circularly polarized luminescence (CPL) dyes have been developed as nextgeneration chiroptical materials. Helicenes, ortho-fused aromatics, have been recognized as some of the most promising CPL dyes. Although typical carbohelicenes show CPL, weak fluorescence is often emitted in the blue region. In contrast, heteroatom-embedded helicenes (heterohelicenes) can show intense fluorescence and CPL in the visible region because heteroatoms alter the electronic states of helicene frameworks. Among various heterohelicenes, nitrogen-embedded helicenes (azahelicenes) have unique features such as facile functionalization and sensitive responses to acid/base or metal ions. Furthermore, polycyclic aromatic hydrocarbons (PAHs) containing azaborine units have been recognized as excellent luminescent materials, and the helical derivatives, B,N-embedded helicenes, have been rapidly growing recently. In this feature article, we review and summarize the synthesis and chiroptical properties of azahelicenes, which are classified into imine-type and amine-type azahelicenes and B,Nembedded helicenes. CPL switching systems of azahelicenes are also reviewed.

1. Introduction

Circularly polarized luminescence (CPL) is associated with the difference in intensities of the left-handed (I_L) and righthanded circularly polarized light (I_R) , and CPL-active dyes have been actively studied for their potential application in 3D displays, security paints, information storage, and optical communications.1 CPL is generally evaluated using the luminescence dissymmetry factor, g_{lum} , defined as $2(I_L - I_R)/(I_L + I_R)$. A variety of chiral organic molecules and metal complexes with high g_{lum} values have been developed, although it has often been difficult to achieve high values of both fluorescence quantum yield (Φ_F) and g_{lum} . Recently, CPL brightness (B_{CPL}) defined as $\varepsilon \times \Phi_{\rm F} \times g_{\rm lum}/2$ has also been used to quantify the whole chiroptical performance including the molar extinction coefficient (ε) and $\Phi_{\rm F}$ along with $g_{\rm lum}$. ¹

Helicenes are polycyclic aromatic hydrocarbons (PAHs) consisting of ortho-fused aromatic rings showing chiroptical properties derived from inherent helical chirality and have been recognized as some of the most promising CPL dyes.2 Although general carbohelicenes exhibit CPL, their fluorescence is often weak and emitted in the blue region. In addition, CPL and circular dichroism (CD) are more sensitive to substituents than to helical sense.3 On the other hand, the incorporation of heteroatoms into helicene frameworks can modulate the

Division of Applied Chemistry, Graduate School of Natural Science and Technology, Okayama University, Tsushima, Okayama 700-8530, Japan. E-mail: cmaeda@okayama-u.ac.jp, ema@cc.okayama-u.ac.jp

electronic states, and such heteroatom-embedded helicenes (heterohelicenes) show intense fluorescence and CPL in the visible to near infrared (NIR) region. Among the heterohelicenes, nitrogen-embedded helicenes (azahelicenes) have attracted considerable attention due to easy functionalization and derivatization and possible mutual interactions such as hydrogen bonding and metal coordination.

Azahelicenes can be classified into imine-type and aminetype (Fig. 1). The former often contains a pyridine ring, while the latter usually contains a pyrrole or carbazole ring. Iminetype nitrogen allows protonation to generate cationic species or coordination with metal ions, which enables a pH- or coordination-driven chiroptical switching. Amine-type nitrogen allows various functionalizations such as alkylation, arylation, borylation, and metal complexation, and such azahelicenes function as a chiral electron-donating unit.

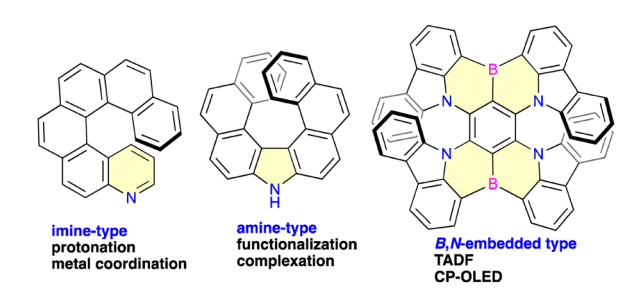


Fig. 1 Classification of nitrogen-embedded helicenes in this article.

Azaborines contain both nitrogen and boron atoms in an aromatic six-membered ring in place of two carbon atoms and have unique electronic states, aromaticity, and reactivities.⁴ Recently, PAHs containing azaborine unit(s) have been recognized as excellent luminescent materials such as thermally activated delayed fluorescence (TADF) emitters and organic light-emitting diodes (OLEDs).^{4c-e} Very recently, helicenes with azaborine unit(s) have been actively studied for their potential application as chiral TADF materials and in CP-OLEDs.

Here, we summarize recent advances in CPL-active azahelicenes, classifying them into imine-type and amine-type azahelicenes and B,N-embedded helicenes containing azaborine units (Fig. 1). The key synthetic schemes to obtain azahelicenes and examples of CPL switching are highlighted.

2. Synthesis and CPL properties of azahelicenes

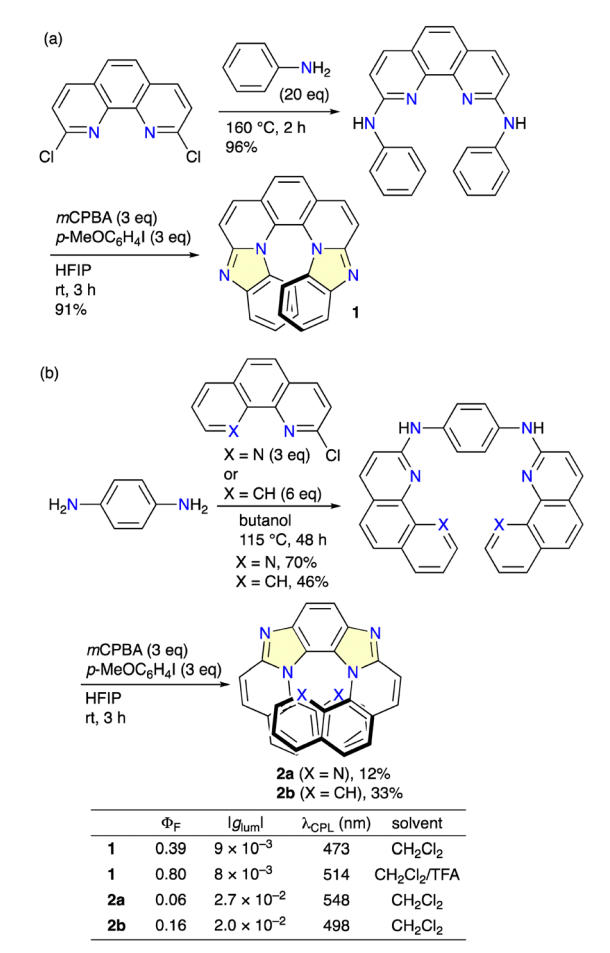
Although the distortion of helicenes sometimes hinders the synthesis, extensive and intensive efforts have been devoted to the development of synthetic methods for a variety of helicenes including long helicenes, multiple helicenes, and cationic helicenes. In this section, the synthesis of CPL-active azahelicenes is summarized. Some examples of the enantioselective synthesis are also highlighted.

2.1. Azahelicenes with imine-type nitrogen

Otani, Shibata, and co-workers developed the facile two-step synthesis of tetraaza[7]helicene 1 from 2,9-dichloro-1,10phenanthroline via the double amination reaction followed by hypervalent iodine-mediated intramolecular coupling (Scheme 1a).5a Racemate 1 was resolved by means of HPLC with a CHIRALCEL OD stationary phase into each enantiomer showing fluorescence and CPL with $\Phi_{\rm F}$ and $|g_{\rm lum}|$ values of 0.39 and 9×10^{-3} , respectively. Interestingly, the $\Phi_{\rm F}$ value increased to 0.80 upon protonation with TFA. The same group also synthesized polyaza[9]helicenes 2a and 2b via the reaction of p-phenylenediamine with 2-chloro-1,10-phenanthroline or 2-chlorobenzoquinoline followed by intramolecular coupling (Scheme 1b). 5b 2a and 2b showed even higher $|g_{lum}|$ values of 2.7×10^{-2} and 2.0×10^{-2} , respectively. The redshifted CPL suggests the structural change or aggregation in the excited state, which might contribute to large $|g_{lum}|$ values.

Mori, Miura, and co-workers reported the two-step synthesis of tetraaza[7]helicene 3 from indolocarbazole via direct arylation with 2-bromo-6-phenylpyridine, followed by dehydrogenative intramolecular coupling (Scheme 2). Racemic compound 3 was resolved by means of HPLC using a YMC CHIRAL ART amylose-SA stationary phase into each enantiomer showing CPL with a $|g_{lum}|$ value of 4.4×10^{-3} at 429 nm, which increased to 5.8×10^{-3} at 509 nm upon protonation.

Gu and co-workers reported a ring-expansion strategy for the synthesis of α -aryl aza[7]helicene 4 *via* the acid-mediated reaction of helical dinaphthofluoren-9-ols with NaN₃ (Scheme 3).⁷ The reaction mechanism was proposed as follows. Carbocation



Scheme 1 Synthesis of polyazahelicenes (a) 1 and (b) 2.

Scheme 2 Synthesis of tetraaza[7]helicene 3

Int-1 is generated *via* the protonation of the tertiary alcohol. Azido fluorene **Int-2** was formed *via* S_N1 type substitution. Subsequently, 1,2-migration/ring expansion occurs with the release of N_2 to deliver N-heterocyclic cation species **Int-3**. Finally, aromatization/deprotonation of **Int-3** produces azahelicene **4**. Because the tertiary alcohols could be readily prepared

	R	Φ_{F}	$ g_{lum} $	$B_{\rm CPL} ({\rm M}^{-1} {\rm cm}^{-1})$	solvent
4a	Ph	0.060	2.2×10^{-3}	1.53	CH ₂ Cl ₂
4b	4-MeO-C ₆ H ₄	0.052	4.5×10^{-3}	1.98	CH ₂ Cl ₂
4c	4-Br-C ₆ H ₄	0.064	2.7×10^{-3}	1.47	CH ₂ Cl ₂
4d	7- ^t Bu-pyren-2-yl	0.073	3.0×10^{-3}	7.39	CH ₂ Cl ₂

Scheme 3 Synthesis of α -aryl aza[7]helicenes 4 via the acid-mediated ring-expansion strategy

by the reactions of helical ketones with Grignard reagents or organolithiums, a variety of azahelicenes were obtained. The azahelicenes showed CPL at around 490 nm with $|g_{lum}|$ values of $2.2-4.5 \times 10^{-3}$.

Lacour and co-workers have investigated the synthesis and chiroptical properties of cationic azahelicenes 5, which are of particular interest due to the chemical and configurational stabilities, easy preparation, and chiroptical properties in up to the far-red region (Fig. 2).8 Functionalization of the 6-position produced various cationic azahelicenes with tunable chiroptical properties, and CPL was recorded in the red region with a $|g_{\text{lum}}|$ value of ca. 1×10^{-3} .8a The authors also synthesized oligoacene-incorporated azahelicene 6 showing CPL at

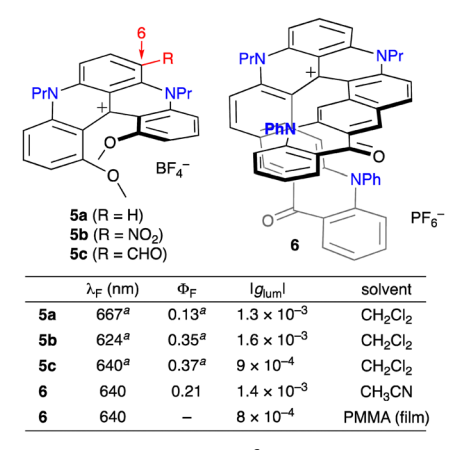


Fig. 2 Cationic azahelicenes 5 and 6. a In CH3CN.

$$\begin{array}{c} \text{1. POCl}_3 \, (2 \, \text{eq}) \\ \text{DMF} \\ \text{90 °C, 3 h} \\ \text{32\%} \\ \text{2. NH}_4 \text{PF}_6 \\ \text{CH}_2 \text{Cl}_2 / \text{MeOH} \\ \text{quant} \\ \\ \hline \\ \text{0.08} \quad 6.0 \times 10^{-3} \quad 685 \quad \text{CHCl}_3 \\ \text{0.01} \quad 6.0 \times 10^{-3} \quad 690 \quad \text{H}_2 \text{O/MeOH (9/1)} \\ \end{array}$$

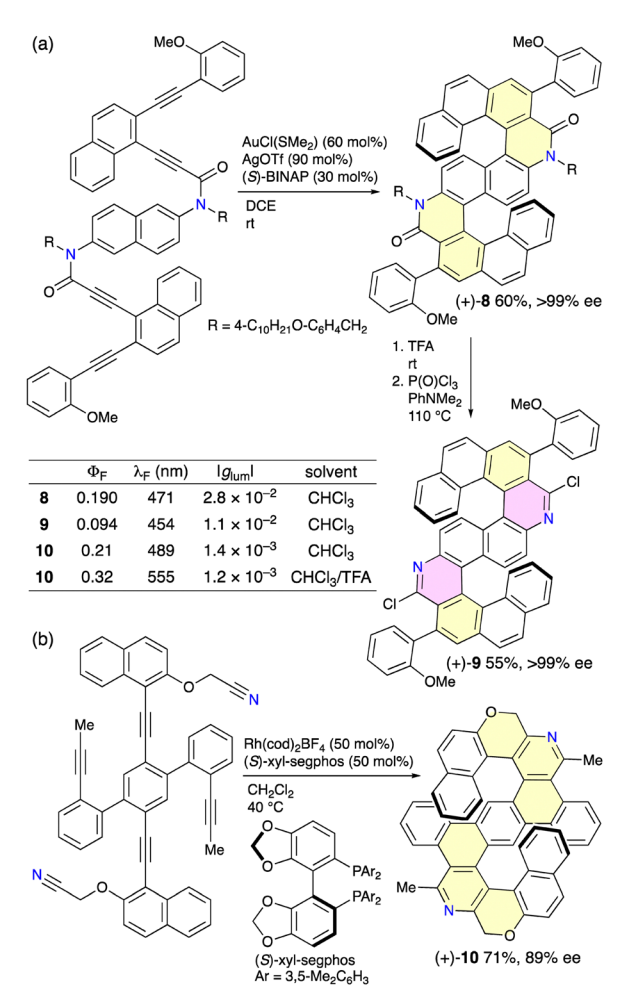
Synthesis of phenanthrene-fused cationic aza[7]helicene 7.

640 nm both in acetonitrile solution and in the PMMA film with $|g_{\text{lum}}|$ values of 1.4 \times 10⁻³ and 8 \times 10⁻⁴, respectively. 8c

Olivier, Ferrand, and co-workers synthesized phenanthrenefused cationic aza[7]helicene 7 (Scheme 4). When bis(benzo[c]phenanthren-2-yl)phenylamine was treated under Vilsmeier-Haack conditions, intramolecular cycloaromatization and simultaneous quaternarization occurred to form the dibenzoacridinium derivative, and the subsequent intramolecular dehydrogenative C-C coupling between one of the phenanthrene units and the neighboring pyridinium ring took place leading to the formation of 7. 7 was soluble both in organic and aqueous media $(H_2O/MeOH = 9/1)$ and showed CPL with $|g_{lum}|$ values of 6×10^{-3} in both media after the optical resolution by means of HPLC on a CHIRALPAK IA stationary phase.

The development of efficient methods for the enantioselective synthesis of heterohelicenes is important and challenging. Tanaka and co-workers achieved the enantioselective synthesis of S-shaped double azahelicenes (Scheme 5). 10 The gold-catalyzed sequential intramolecular hydroarylation of alkynes in the presence of AgOTf and (S)- or (R)-BINAP produced S-shaped double azahelicene 8 in 60% yield with an enantiomeric excess (ee) of >99% (Scheme 5a). 10a Removal of the 4-alkoxybenzyl groups on the nitrogen atoms followed by chlorination afforded double azahelicene 9 possessing two pyridine units without racemization. 8 and 9 showed intense CPL with $|g_{lum}|$ values of 2.8×10^{-2} and 1.1×10^{-2} , respectively. The authors also reported the rhodium-catalyzed intramolecular [2+2+2] cycloaddition of cyanodiynes in the presence of (S)-xyl-segphos giving S-shaped double azahelicene-like molecule 10 in 71% yield with 89% ee (Scheme 5b). 10 showed fluorescence at 489 nm with a $\Phi_{\rm F}$ value of 0.21, which increased to 0.32 at 555 nm upon protonation with TFA. 10 is also CPL-active with $|g_{\text{lum}}|$ values of 1.4×10^{-3} in the neutral state and 1.2×10^{-3} in the cationic state.

Zhong, Luo, Zhu, and co-workers achieved the palladiumcatalyzed modular synthesis of pyridohelicenes through double cyclization reactions, and a variety of pyrido[6]helicenes and furan-containing pyrido[7]helicenes were obtained by the enantioselective reactions of diisocyanides with aryl iodides.¹¹ A representative example is shown in Scheme 6. (P)-/(M)-Enantiomers of 11 exhibited mirror-image CD spectra with absorption dissymmetry factors ($g_{\rm abs}$) of +3.9/–5.0 imes 10⁻³ at 340 nm, and they also exhibited mirror-image CPL with a $|g_{lum}|$ value of 6.25×10^{-4} at 430 nm. The origin of enantioselectivity



Scheme 5 Enantioselective synthesis of double azahelicenes (a) **8**, **9**, and (b) **10**.

Scheme 6 Enantioselective synthesis of pyrido[6]helicene 11.

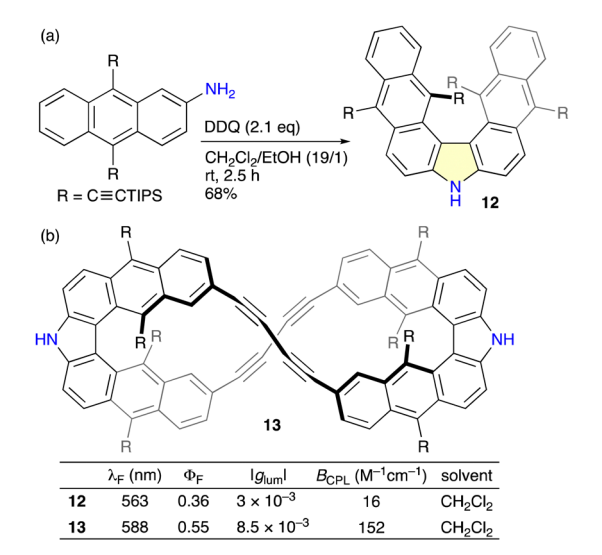
was studied by DFT calculations on the second pyridine ring formation. A pivalate ion-assisted concerted metalation-deprotonation (CMD) takes place in the enantioselectivity-determining step. The formation of the major enantiomer is 3.4 kcal mol⁻¹ more favorable than that of the minor enantiomer. This calculated energy difference corresponds to 98% ee,

which agrees with the experimental result (98% ee). Clearly, this energy difference in the C–H bond activation is the key to the highly enantioselective reaction.

2.2. Azahelicenes with amine-type nitrogen

Carbazole is known as a planar tricyclic aromatic showing highly emissive and electron-conducting abilities and chemical stabilities. From another viewpoint, carbazole can be regarded as an aza[3]helicene, and π -extension at the 3,4- and 5,6positions leads to aza[n]helicenes showing chiroptical properties. Hiroto, Shinokubo, and co-workers developed the synthesis of aza[5]helicene 12 via the oxidative coupling of a 2-aminoanthracene derivative with DDQ in the presence of EtOH (Scheme 7a). Thanks to the bulky triisopropylsilyl groups, optically active compound 12 was resolved by means of HPLC using a CHIRALPAK IA stationary phase and showed fluorescence and CPL with a $\Phi_{\rm F}$ value of 0.36 and a $|g_{\rm lum}|$ value of 3 \times 10⁻³. The same group also synthesized figure-eight aza[5]helicene dimer 13 showing more intense CPL with a $\Phi_{\rm F}$ value of 0.58 and a $|g_{\text{lum}}|$ value of 8.5 \times 10⁻³, and the B_{CPL} reached 152 M⁻¹ cm⁻¹ (Scheme 7b). 12b

The photocyclization of 3,6-bis(styryl)carbazoles giving aza[7]helicenes is an efficient and practical method because the substrates are readily prepared via the Mizoroki–Heck reaction of 3,6-dihalogenated carbazoles (Scheme 8).¹³ On the other hand, similar aza[7]helicenes were also synthesized via the double amination reaction¹⁴ or S_NAr reaction of thia[7]helicene S_iS_i -dioxides.¹⁵ Nakano and co-workers investigated the chiroptical properties of **14a** and **14b**, and $|g_{abs}|$ and $|g_{lum}|$ values of 4×10^{-3} were recorded.¹⁵ Wang, Wang, and co-workers found that tetramethyl-substituted aza[7]helicene **14c** showed an enhanced racemization barrier and chiroptical performance with a $|g_{lum}|$ value of 3.1×10^{-3} as compared to unsubstituted aza[7]helicene **14d** (2.0×10^{-3}) .^{14c}



Scheme 7 (a) Synthesis of aza[5]helicene 12. (b) Figure-eight aza[5]helicene dimer 13.

ChemComm Feature Article were enhanced by the attachment of axial chirality. Interest-

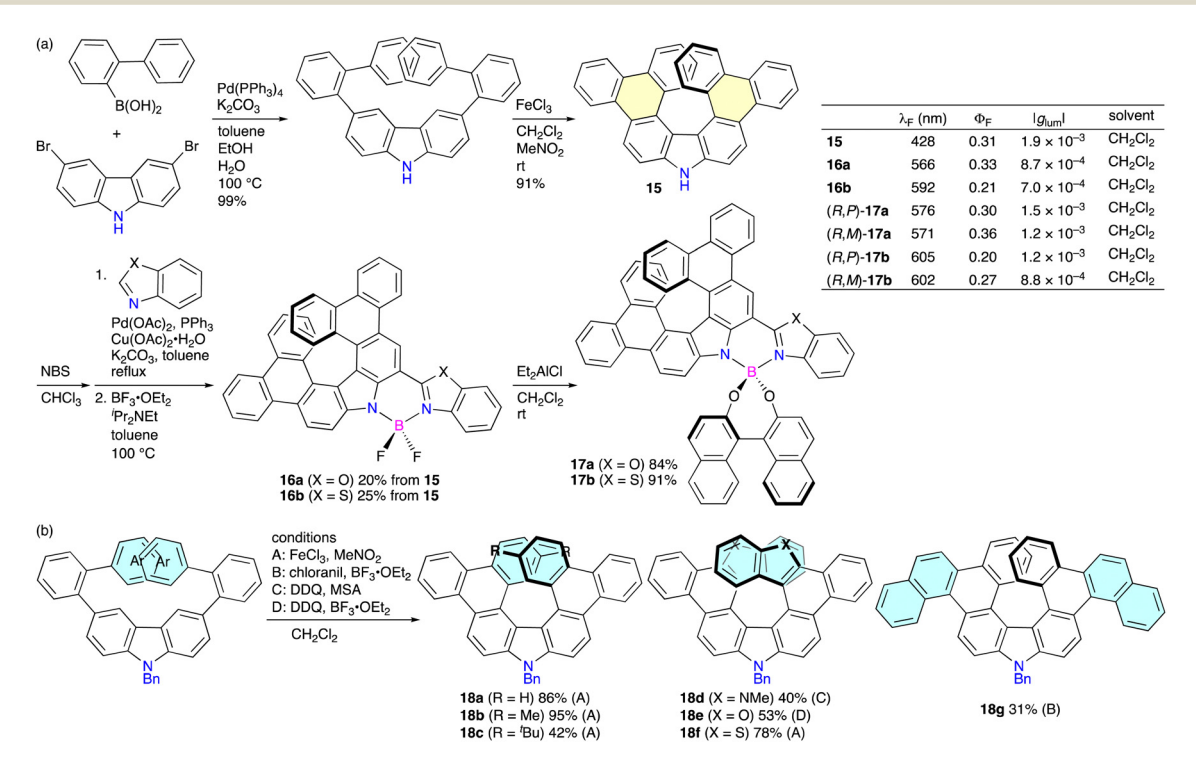
Ar
$$\frac{\text{Ar}}{\text{NR}}$$
 $\frac{\text{NR}}{\text{NR}}$ $\frac{\text{NR}}{\text{NR}}$ $\frac{\text{NR}}{\text{N}}$ $\frac{\text{NR}}{\text{N}}$

Synthesis of aza[7]helicene 14. aln CH2Cl2

Maeda, Ema, and co-workers developed the facile synthesis of aza[7]helicene 15 via the intramolecular oxidative aromatic coupling of 3,6-bis(1,1'-biphenyl-2-yl)carbazole (Scheme 9a). 16a Attachment of benzoxazole or benzothiazole to 15, followed by the boron complexation produced chiral BODIPY analogues **16a** and **16b** showing CPL with g_{lum} values of 8.7 \times 10⁻⁴ and 7.0×10^{-4} , respectively. Furthermore, (R)-BINOL was attached to the boron atom via the Et₂AlCl-mediated reaction developed by the same group. 17 The chiroptical properties of 17a and 17b

ingly, the (R,P)-diastereomers showed somewhat higher g_{lum} values $(-1.5 \times 10^{-3}/-1.2 \times 10^{-3} \text{ for } 17a/17b)$ than the (R,M)diastereomers (+1.2 \times 10⁻³/+8.8 \times 10⁻⁴ for 17a/17b), suggesting the enhancement effect of chirality by the (P)-azahelicene and (R)-binaphthyl group. They also investigated the oxidative aromatic coupling of several 3,6-bis(2-arylphenyl)carbazoles, and the corresponding aza[7]helicenes 18a-c and hetero[9]helicenes **18d-f** were synthesized (Scheme 9b). ^{16b} Interestingly, triple helicene 18g was obtained from the 3,6-bis(2-naphthylphenyl)carbazole via double rearrangement. This rearrangement was controlled by the N-substituents of the carbazoles; Similar rearrangement products were obtained from the N-ethyl and N-4-tert-butylphenyl carbazoles, while the aza[9]helicene was obtained from the N-benzoyl carbazole. 16c These azahelicenes showed CPL with $|g_{lum}|$ values in the range of 2.9 \times 10⁻⁴ -3.5×10^{-3} .

Because of the synthetic ease and potential applications as a chiral electron-donating unit, azahelicene 15 was also used by other groups. 18-21 Wang and co-workers synthesized donoracceptor (D-A) type CPL materials 19 composed of azahelicene 15 and triphenyltriazine (Fig. 3a). 18 DFT calculations of 19a suggested that the magnitude of the transition dipole moment $|\mu|$ and magnetic dipole moment |m| was highly dependent on the dihedral angle (ϕ) of the D–A moiety and that the minimum $|\mu|$ value was calculated at a ϕ value of 105°. Because the μ and m were aligned in parallel at any ϕ , a maximum g_{lum} was expected at 105°. Based on the calculations, 19b with two methyl groups was also prepared since the ϕ value of the calculated structure of 19b was 92°, close to the ideal value of



Scheme 9 (a) Synthesis of aza[7]helicene 15 and derivatized boron complexes 16 and 17. (b) Synthesis of aza[7]helicenes and aza[9]helicenes 18

Fig. 3 Aza[7]helicene functionalized (a) triphenyltriazines 19 and (b) triphenylmethyl radicals 20

105°. **19a** and **19b** showed similar CPL responses at 390–500 nm, while **19b** showed a higher $|g_{\text{lum}}|$ value of 3.5×10^{-3} than **19a** (2.1×10^{-3}) . This work provides a new insight to boost the $|g_{\text{lum}}|$ value of D–A type CPL materials by modulating the dihedral angle (ϕ) .

Ravat, Kuehne, and co-workers synthesized aza[7]helicenes **20** functionalized with triphenylmethyl radicals via the Buchwald–Hartwig amination of iodinated-tris(2,4,6-trichlorophenyl)methyl radical with **14d** or **15** (Fig. 3b).¹⁹ These radicals were stable enough to be isolated and resolved into the enantiomers. **20a** and **20b** displayed broad absorption bands at around 650 nm originating from the transition of the highest occupied molecular orbital (HOMO) to singly occupied molecular orbital (SOMO) and fluorescence at around 700 nm with $\Phi_{\rm F}$ values of ca. 0.4. Optically active **20a** showed CPL with a $|g_{\rm lum}|$ value of 5.0×10^{-4} , while **20b** was CPL-inactive under the measurement conditions.

Zhang, Chen, and co-workers synthesized double aza[7]helicene 21 via the KMnO₄-mediated N-N coupling of the brominated aza[7]helicene, followed by the Yamamoto coupling (Scheme 10).²⁰ 21 showed a relatively weak absorption band at 560 nm probably due to the existence of the central N2C4 core with antiaromatic character. Optical resolution of 21 was performed by means of HPLC using a CHIRALPAK IA-3 stationary phase to furnish (P,P)-21 and (M,M)-21 showing mirror-imaged CD along with the achiral compound (P,M)-21. The optically active compound (P,P)-21 showed red CPL with a $\Phi_{\rm F}$ value of 0.86, a $|g_{\rm lum}|$ value of 2.2 \times 10⁻⁴, and a $B_{\rm CPL}$ value of 13.2 M⁻¹ cm⁻¹. 21 also showed solid-state fluorescence with a $\Phi_{\rm F}$ value of 0.10, and CPL was recorded in the film state with a $|g_{\text{lum}}|$ value of 2.0 × 10⁻⁴. Furthermore, cyclic voltammetry (CV) measurements of 21 revealed two reversible one-electron oxidation waves at +0.30 and +0.73 V (vs. Fc^+/Fc in CH_2Cl_2). Hence, chemical oxidation of 21 was also conducted using NOSbF₆, which generated radical cation 21°+ and dication 212+ in two steps. Nucleus-independent chemical shift (NICS) values of the central N2C4 core were calculated to be +9.25 and -10.68 for 21 and 212+, respectively, indicating switching from antiaromaticity

Scheme 10 Synthesis of double aza[7]helicene 21.

to aromaticity character. This aromaticity and antiaromaticity switching was further supported by the anisotropy of the induced current density (ACID) calculations and harmonic oscillator model of aromaticity (HOMA) values.

Li, Jin, Chen, and co-workers synthesized triphenylamine-bridged aza[7]helicene dimer 22 via the Suzuki-Miyaura coupling of racemic dibromoaza[7]helicene and triphenylamine 4,4'-diboronic acid pinacol ester (Scheme 11).²¹ Interestingly, meso compound (P,M)-22 was not detected. Optical resolution of 22 was performed by means of HPLC on a CHIRALPAK IG-3 stationary phase to furnish (P,P)-22 and (M,M)-22 showing

Scheme 11 Synthesis of triphenylamine-bridged aza[7]helicene dimer 22.

mirror-imaged CD with a $|g_{abs}|$ value of 2.5 \times 10⁻³ at 435 nm and CPL with a $|g_{lum}|$ value of 5.0 \times 10⁻³ at 460 nm. The $\Phi_{\rm F}$ value was nearly quantitative (0.99), and the $B_{\rm CPL}$ value reached 100 M⁻¹ cm⁻¹. Furthermore, the chemical oxidation of electron-rich chiral macrocycle 22 with NOSbF₆ generated a tetraradical cation species as confirmed by the UV/vis-NIR absorption and ESR spectroscopy.

Casado, Liu, and co-workers prepared hexa-peri-hexabenzocoronene (HBC)-fused aza[7]helicene 23 (Fig. 4).22 23 adopts a twist-helix geometry, while the energy barrier for racemization dramatically increases to 143 kcal mol⁻¹, which is much higher than the value of typical aza[7]helicenes such as 15 (ca. 30 kcal mol⁻¹). 23 exhibited excellent chiroptical properties

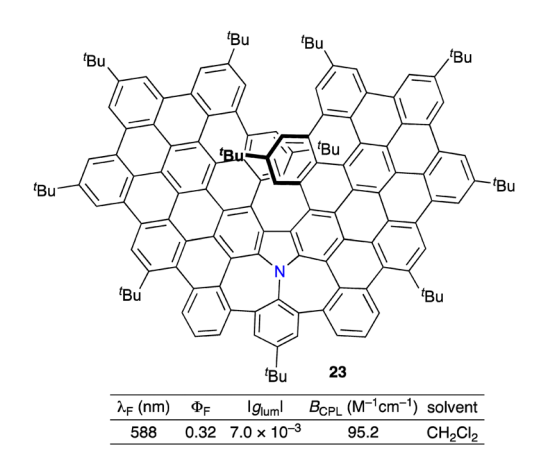
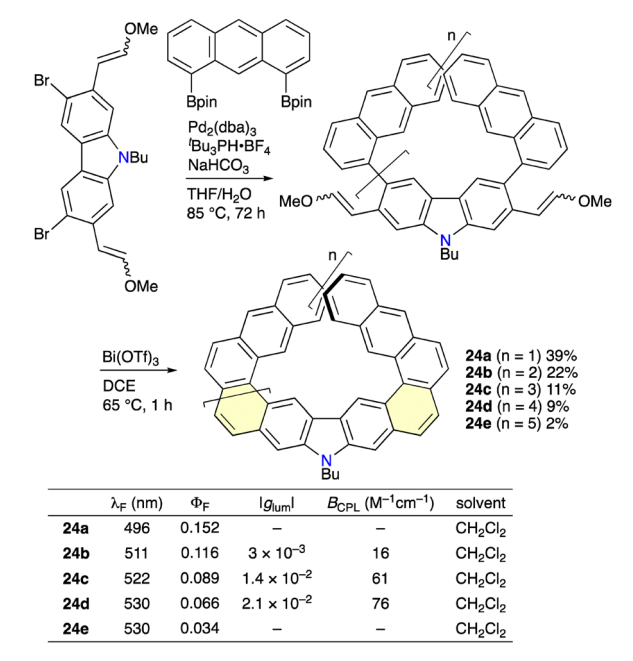


Fig. 4 Structure of π -extended aza[7]helicene 23

with a $|g_{abs}|$ value of 1.0×10^{-2} , a $|g_{lum}|$ value of 7.0×10^{-3} , and a B_{CPL} value of 95.2 M⁻¹ cm⁻¹.

Expanded helicenes, which are defined as helicene analogues containing linearly fused aromatic rings in the helical structures, are promising candidates for molecular springs due to their large helical diameter. However, the optical resolution has rarely been achieved because of the low racemization barrier. In addition, it is also difficult to achieve high g_{lum} values due to the flexible structures in the excited state. Yang, Wu, and co-workers reported the synthesis of expanded azahelicenes 24a-e consisting of up to 43 fused rings via the Suzuki-Miyaura coupling of 3,6-dibromo-2,7-bis(2-methoxyvinyl)carbazole and anthracene 1,8-diboronic ester and the subsequent Bi(OTf)₃-catalyzed cyclization (Scheme 12).^{23a} 24ae were obtained in 81% total yields in two steps and easily separated by means of gel permeation chromatography (GPC). 24b-d were characterized by X-ray diffraction analysis and resolved by means of HPLC on a CHIRALPAK IG stationary phase into each enantiomer. They showed CPL with $|g_{lum}|$ and $B_{\rm CPL}$ values of up to 2.1 \times 10⁻² and 76 M⁻¹ cm⁻¹, respectively, which are superior to the all-carbon counterparts.^{23b}

It is quite challenging to synthesize longer helicenes. Tanaka and co-workers reported the synthesis of benzannulated aza[n]helicenes 25a-f (n = 9-19) via the one-shot oxidative fusion reaction of ortho-phenylene-bridged oligopyrroles with PIFA (Scheme 13a). The structures of all the aza[n]helicenes were characterized by X-ray diffraction analysis, which revealed the triple-layer helixes of the aza[17]helicene and aza[19]helicene for the first time. 25a-d were butylated with an excess amount of butyl iodide, and the optical resolution of the N-butylated azahelicenes was determined to give two fractions showing mirror-imaged CD and CPL spectra with $|g_{\text{lum}}|$ values of 1.7-5.7 \times 10⁻³ in THF. The same group also



Scheme 12 Synthesis of expanded azahelicenes 24a-e.

25d-Bu 12%

Scheme 13 (a) Synthesis of benzannulated aza[n] helicenes 25 up to n = 19. (b) Benzannulated double aza[9] helicenes 26

reported the two-step synthesis of benzannulated double aza[9]helicenes via the Suzuki-Miyaura coupling of 1,2,4,5tetrabromobenzene and 5-{2-(indol-2-yl)phenyl}pyrrole 2boronic ester and the subsequent oxidative fusion reaction using PIFA.24b Optical resolution of N-alkylated double aza[9]helicenes 26-Et and 26-Bu was achieved, and the optically active double helicenes showed fluorescence and CPL with $\Phi_{ extsf{F}}$ and $|g_{\text{lum}}|$ values of 0.35 and 1 \times 10⁻³, respectively (Scheme 13b).

Hu and co-workers reported the two-step synthesis of double aza[7]helicene 27 via the Suzuki-Miyaura coupling of 4,4"-ditert-butyl-2,2",6,6"-tetrabromo-p-terphenyl and 9-phenylcarbazole-2-boronic acid and the subsequent Scholl reaction using DDQ/TfOH (Scheme 14).25 Interestingly, the use of a larger amount of DDQ or the further reaction of 27 furnished azananographene 28 with two octagons, which bound C₆₀ and C₇₀ with binding constants (K_a) of 9.5 \times 10³ and 3.7 \times 10⁴ M⁻¹, respectively. DFT calculations and VT-NMR analysis indicated the fast racemization of 28 at rt, while 27 was resolved by means of HPLC on a CHIRALPAK IE stationary phase into each enantiomer showing fluorescence and CPL with $\Phi_{\rm F}$ and $|g_{\rm lum}|$ values of 0.45 and 2.4 \times 10⁻³, respectively. The $B_{\rm CPL}$ was calculated to be 173 M⁻¹ cm⁻¹, which was among the highest values for ever-reported helical molecules.

Ito, Jin, and co-workers demonstrated the crystallineinduced chirality transfer in conformationally flexible aza[5]helicene Au(1) complexes inducing CPL (Scheme 15).²⁶ Chiral NHC Au(1) complexes (S,S)- and (R,R)-29 were obtained from (S,S)- or (R,R)-NHC Au(1) chloride and aza[5]helicene in 96% and 92%, respectively. (S,S)-29 exhibited dynamic chirality in the aza[5]helicene moiety because of the low flipping barrier, and CPL was inactive in solution. In sharp contrast, the chiral diphenyl moieties of the (S,S)-NHC ligand interacted with the aza[5]helicene unit of another complex in the crystal to induce

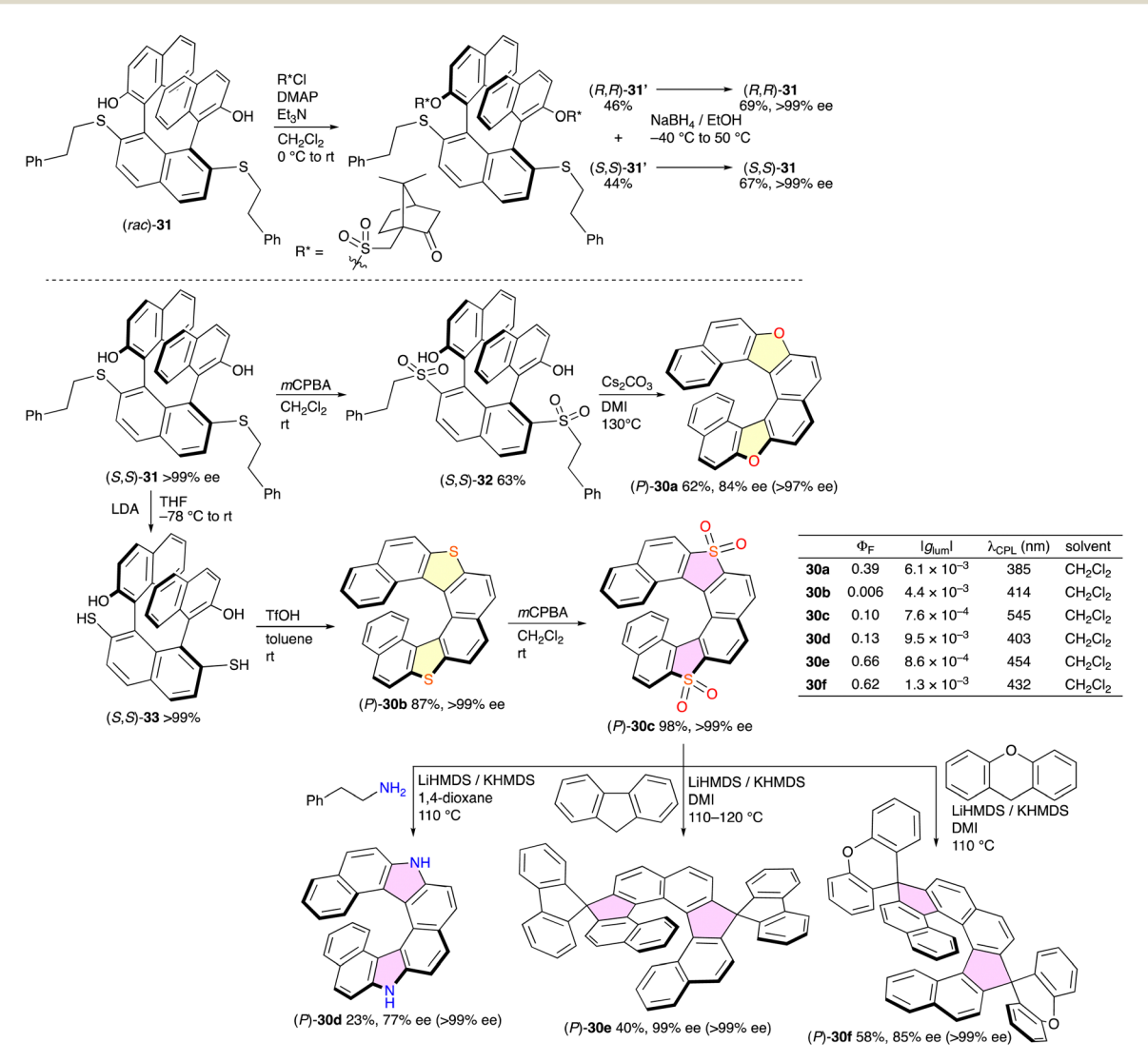
Scheme 14 Synthesis of double aza[7]helicene 27 and azananographene 28

(M)-chirality in the aza[5]helicene, and the crystal showed CPL at 390-470 nm with a $|g_{\text{lum}}|$ value of 3 \times 10⁻³.

As shown above, most of the optically active azahelicenes were resolved by means of chiral HPLC on a small scale. Therefore, the development of the efficient preparation of

Crystalline-induced chirality transfer in the aza[5]helicene Au(i) complex (S,S)-29. R = 3,5-di-tert-butylbenzyl.

optically active helicenes has been desired for wide applications. Diastereomer methods are one of the promising strategies to separate (P)- and (M)-diastereomers of helicenes or their precursors by silica gel chromatography. Yorimitsu and coworkers reported the systematic asymmetric synthesis of dihetero[8]helicenes 30 from common intermediate 31, which was resolved into optically active species by the diastereomer method (Scheme 16).27 Treatment of (rac)-31 with (+)-10camphorsulfonyl chloride gave diastereomers 31', which were successfully separated by silica gel chromatography into (S,S)-31' and (R,R)-31'. The sulfonyl groups could be removed with NaBH₄. The optically active 31 was converted into bis-sulfone 32 and dithiol 33, and the subsequent cyclization reactions of 32 and 33 furnished dioxa[8]helicene 30a and dithia[8]helicene 30b, respectively. Dithia[8]helicene 30b was oxidized to the corresponding tetraoxide 30c, which was further converted into diaza[8]helicene 30d and spiro-shaped helicenes 30e and 30f. Importantly, the enantiopurities were mostly retained, and these dihetero[8]helicenes were obtained in enantiomerically



Scheme 16 Synthetic routes to dihetero[8]helicenes 30a-f. Values of ee in parenthesis are those after recrystallization.

Scheme 17 Synthesis of diastereomeric aza[7]helicenes and conversions into cyclic aza[7]helicene dimers 34 and 35

pure forms (>97% ee). These [8]helicenes were CPL-active with the $|g_{\rm lum}|$ in the range of 7.6 \times 10⁻⁴–9.5 \times 10⁻³, among which diaza[8]helicene **30d** recorded the highest $|g_{\rm lum}|$ value of 9.5 \times 10⁻³ with a $\Phi_{\rm F}$ value of 0.13.

Maeda, Ema, and co-workers prepared diastereomeric azahelicenes with (1R)-menthylcarbonate groups (Scheme 17). The azahelicenes and closed azahelicenes were selectively synthesized under different conditions of the Scholl reactions, and the (P)- and (M)-diastereomers were separated by silica gel chromatography. The optically active aza[7]helicenes were converted into the corresponding butadiyne-bridged dimers (P,P)- or (M,M)-34 and 35 showing CPL with $B_{\rm CPL}$ values of 17–31 ${\rm M}^{-1}$ cm⁻¹, which were higher than the corresponding monomers $(2.3-6.7~{\rm M}^{-1}~{\rm cm}^{-1})$. Furthermore, 34 and 35 were found to recognize a fluoride ion selectively with binding constants $(K_{\rm a})$ of up to $2.0\times10^5~{\rm M}^{-1}$, which induced fluorescence and CPL in the red region.

Chen, Zhou, and co-workers reported an organocatalytic central-to-helical chirality conversion strategy for the enantio-selective synthesis of indolohelicenes. The best chiral phosphoric acid (CPA) was selected for the cycloaddition-elimination reactions between azonaphthalenes and enecarbamates to give indolohelicenoids in high yields and enantios-electivities. A representative example is shown in Scheme 18. The indolohelicenoid 36 was successfully oxidized with DDQ to give indolohelicene 37. (*P*)-/(*M*)-36 showed two CD signals at around 310 and 390 nm with maximum $g_{\rm abs}$ of +3.0/-2.7 × 10^{-3} at 398 nm, while (*P*)-/(*M*)-37 showed three CD signals at 341, 391, and 415 nm with maximum $g_{\rm abs}$ of +4.2/-2.8 × 10^{-3} at 343 nm. A clear mirror-image relationship was observed for the CPL spectra of (*P*)-/(*M*)-enantiomers with maximum $g_{\rm lum}$ of +9.8/-9.6 × 10^{-4} at 435 nm.

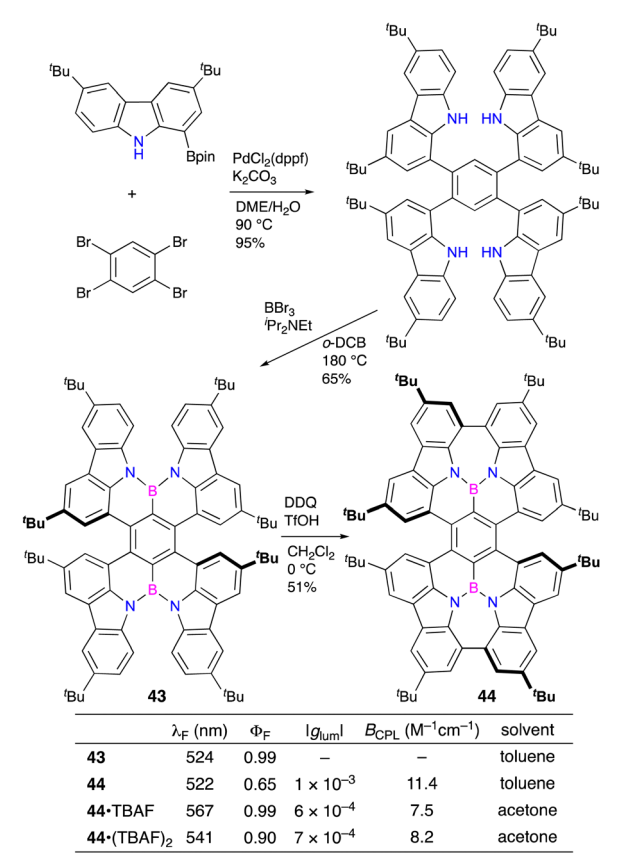
Scheme 18 Enantioselective synthesis of indolohelicenoid 36 and indolohelicene 37.

2.3. B,N-embedded helicenes

Zhang, Duan, and co-workers developed B,N-embedded double helicenes **38a** and **38b** as deep-red emitters for highly efficient OLEDs (Scheme 19). The double helicenes were readily synthesized in two steps from carbazoles and 1,4-dibromo-2,3,5,6-tetrafluorobenzene without using transition metal catalysts. The para-positioned B atoms and N atoms enhance the electronic coupling to allow for the formation of restricted π -bonds on the benzene core for delocalized excited states and a narrow energy gap. In addition, the mutually *ortho*-positioned B and N atoms also induce a multi-resonance effect on the

Scheme 19 Synthesis of B,N-embedded double helicenes 38

peripheral skeleton for non-bonding orbitals, creating shallow potential energy surfaces to suppress the nonradiative transition. The HOMO and LUMO exhibit alternate distribution, which induces a small energy gap between S1 and T1. As a result, 38a and 38b showed efficient TADF emission at 662 nm



Scheme 20 Synthesis of B,N-embedded multiple helicenes 43 and 44.

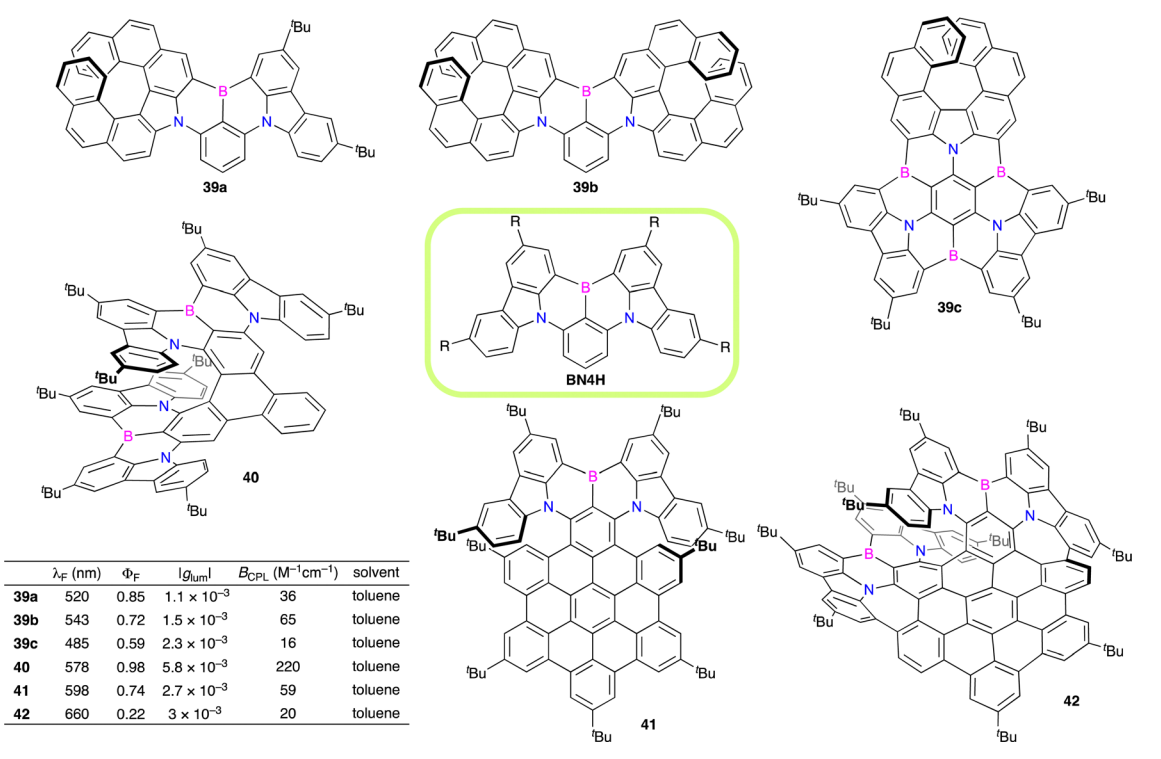


Fig. 5 B,N-embedded helicenes 39-42 containing BN4H segments.

Scheme 21 Synthesis of B,N-embedded [5] and [6]helicenes 45

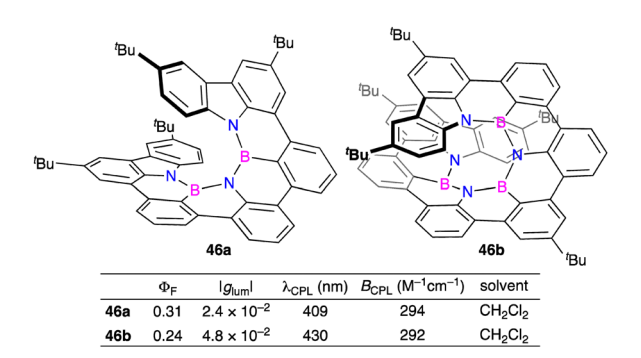


Fig. 6 Benzo-extended heli(aminoborane)s 46a and 46b

and 692 nm with the $\Phi_{\rm F}$ reaching 100%. OLEDs were further constructed to record a maximum external quantum efficiency (EQE) of 28%. Wang and co-workers synthesized **38a-c** to investigate the chiroptical properties. Racemates **38a-c** were resolved by means of HPLC using a CHIRALPAK IE stationary phase into each enantiomer showing CPL with a $|g_{\rm lum}|$ value of 2×10^{-3} . $B_{\rm CPL}$ values of **38a-c** were determined to be 29, 37, and 40 M⁻¹ cm⁻¹, respectively, representing the highest $B_{\rm CPL}$ values in helicenes showing CPL in the red-NIR region.

After the development of **38** with the multi-resonance effect, various CPL-active helicenes containing the B,N-embedded [4]helicene (**BN4H**) segment(s) have been investigated (Fig. 5). Ravat and co-workers developed B,N-embedded helicenes **39a** and **39b** comprising aza[7]helicene in place of the carbazole(s), which showed sharp fluorescence and CPL. Ravat and **39b** showed Φ_F values of 0.85 and 0.72, $|g_{lum}|$ values of 1.1 \times 10⁻³ and 1.5 \times 10⁻³, and B_{CPL} values of 36 and 65 M⁻¹ cm⁻¹, respectively. The fluorescence and CPL bands are narrow (full width at half maximum (FWHM) of 23–28 nm in toluene), which are essential for application to CP-OLEDs. The authors also synthesized **39c** showing ultranarrow band fluorescence (FWHM of 17 nm in toluene) and CPL (FWHM of

18 nm in toluene) with a $\Phi_{\rm F}$ value of 0.59 and $|g_{\rm lum}|$ value of 2.3×10^{-3} .

Li, Chen, and co-workers synthesized B,N-embedded [9]helicene **40**, in which two **BN4H**s were fused to triphenylene. ^{31c} **40** showed bright photoluminescence with a $\Phi_{\rm PL}$ value of 0.98 and CPL with a $|g_{\rm lum}|$ value of 5.8 \times 10⁻³. Furthermore, CP-OLED devices incorporating **40** as an emitter showed a maximum EQE of 35.5%, a small FWHM of 48 nm, and a high $|g_{\rm EL}|$ value of 6.2 \times 10⁻³. The *Q*-factor (EQE \times $|g_{\rm EL}|$) of CP-OLEDs was determined to be 2.2 \times 10⁻³, which was the highest among helicene analogues.

Furthermore, **BN4H**-fused HBCs such as **41** and **42** with TADF character were developed by Tan, Zhang, and co-workers and Liu and co-workers, respectively. ^{31d,e} **41** and **42** showed CPL with $|g_{\text{lum}}|$ values of 2.7×10^{-3} and 3×10^{-3} , respectively. Interestingly, the treatment of **42** with TBAF generated a difluoride adduct with the tetracoordinate borons as confirmed by UV/vis and CD spectroscopy.

Yang and co-workers succeeded in the gram-scale synthesis of multiple helicenes 43 and 44 containing 1,2-azaborine units via the Suzuki-Miyaura coupling of 1,2,4,5-tetrabromobenzene and 3,6-di-tert-butylcarbazole-1-boronic acid pinacol ester and the subsequent boron insertion and the Scholl reaction (Scheme 20). 32 44 adopts a (P,P)- or (M,M)-configuration, and the (P,M)-configuration, less stable by 12.07 kcal mol⁻¹, was not observed. Although the optical resolution of 43 was unsuccessful because of instability, racemate 44 was readily resolved by means of HPLC on a CHIRALPAK ID stationary phase into the enantiomers, which showed fluorescence with a $\Phi_{\rm F}$ value of 0.65 and CPL with a $|g_{\text{lum}}|$ value of 1.0×10^{-3} . Furthermore, 44 underwent the stepwise recognition of fluoride ions to generate monofluoride and difluoride adducts, which also showed CPL. The $\Phi_{\rm F}$ and $|g_{\rm lum}|$ values of the former were 0.99 and 6 \times 10⁻⁴, respectively, while those of the latter were 0.90 and 7×10^{-4} , respectively. Furthermore, the authors confirmed that the addition of BF3·OEt2 to the fluoride adducts regenerated the parent tricoordinate boron species 44.

 $\mathrm{CH_2Cl_2}$

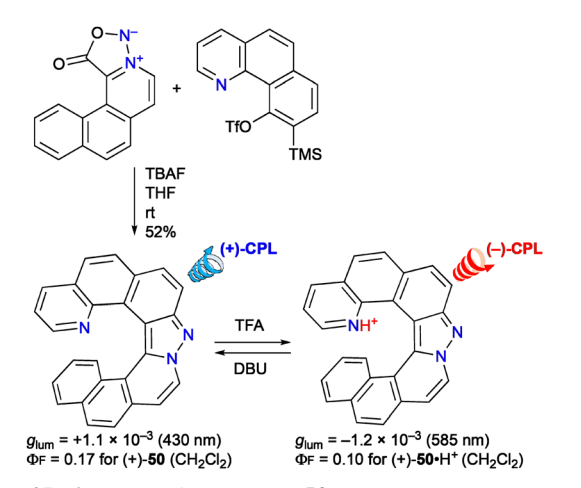
ChemComm

Na₂CO₂ Pt(dmso)₂Me₂ acetone 50 °C

	Φ_{F}	g_{lum}	λ _{CPL} (nm)	solvent
(P)-47	0.084	+3.4 × 10 ⁻³	426	CH ₂ Cl ₂
(P)-47•2H+	0.082	$+3.2 \times 10^{-3}$	590	CH ₂ Cl ₂
(P)-47Pt	0.004	$+1 \times 10^{-3}$	547	CH ₂ Cl ₂
(P)-47Pt•H+	0.027	+1.8 × 10 ⁻³	555	CH ₂ Cl ₂
(P,P)- 48	0.084	$+8.6 \times 10^{-3}$	420	CH ₂ Cl ₂
(P,P)-48•Zn(OAc) ₂	0.19	$+1.2 \times 10^{-3}$	480	CH ₂ Cl ₂
(P,P)- 49	0.22	$+4.8 \times 10^{-3}$	425	CH ₂ Cl ₂
(P,P)-49•Zn(OAc) ₂	0.44	$+1.8 \times 10^{-3}$	495	CH ₂ Cl ₂

HBF₄

Scheme 22 CPL switching systems based on bis(pyridine)-containing aza[6]helicenes (a) 47, (b) 48, and (c) 49. TPEN = N,N,N',N'-tetrakis(2pyridylmethyl)ethane-1,2-diamine



Scheme 23 Synthesis of azahelicene 50 through 1,3-dipolar cycloaddition of sydnones with arynes and the pH-triggered chiroptical switch.

Staubitz and co-workers synthesized [5] and [6]helicenes 45a and 45b comprising two 1,2-azaborine rings via Suzuki-Miyaura coupling and metal-catalyzed cyclization (Scheme 21).³³ 45a had a relatively high racemization barrier ($t_{1/2\text{rac}} \approx 80 \text{ min at } 60 ^{\circ}\text{C}$ and $\Delta G^{\ddagger} = 25.7 \text{ kcal mol}^{-1}$), while racemization of **45b** did not occur even at 200 °C for 14 h. Optical resolution of 45a and 45b was performed by means of HPLC on a CHIRALPAK IA stationary

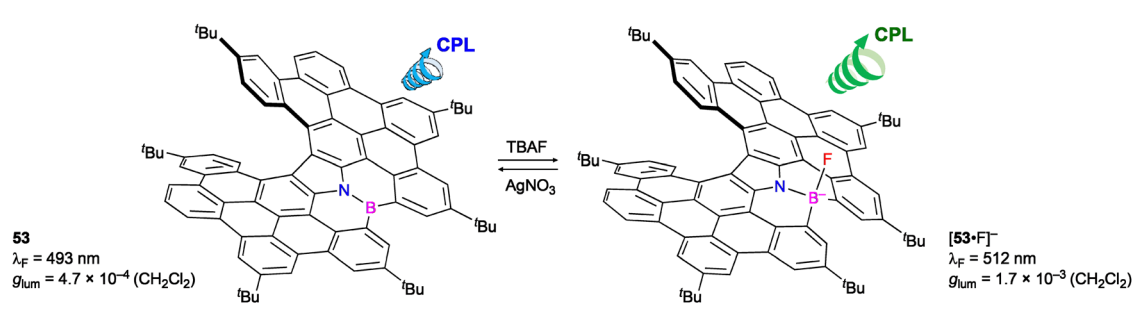
phase into enantiomers showing mirror-imaged CD and CPL with $|g_{\rm abs}|$ and $|g_{\rm lum}|$ values of 9.9×10^{-3} and 4.2×10^{-3} , respectively, for **45a** and 1.1×10^{-2} and 1.3×10^{-2} , respectively for **45b**. The $B_{\rm CPL}$ values of 45a and 45b were 10 and 59 ${\rm M}^{-1}$ cm⁻¹, respectively, which were much higher than those of carbohelicenes despite the similar structural geometries.

Liu and co-workers synthesized benzo-extended heli(aminoborane)s 46a and 46b as a B,N-embedded [8]helicene and [10]helicene, respectively (Fig. 6).³⁴ **46a** and **46b** had significant racemization barriers of 46.92 and 40.61 kcal mol⁻¹, respectively and were resolved by means of HPLC on a CHIRALPAK IF stationary phase into the enantiomers. Optically active compounds 46a and 46b exhibited excellent chiroptical properties with the $|g_{abs}|$ values of 0.036 and 0.061, $|g_{lum}|$ values of 0.024 and 0.048, and B_{CPL} values of 294 and 292 M^{-1} cm⁻¹, respectively.

3. Azahelicenes showing CPL switching

Chiral dyes with multiple interconvertible states can exhibit a chiroptical switch by external stimuli. Although CPL switching systems have been growing in the last decade,35 they are still limited as compared to CD switching systems, especially for

Synthesis of pentaaza[10]circulene 51, closed-azahelicenes 52a-c, and dimers (52b)₂ and (52c)₂



B,N-embedded helicene 53 showing the ion-triggered chiroptical switch

helicene-based ones. Unlike carbohelicenes, azahelicenes are good candidates for CPL switching systems because the nitrogen-containing functional groups can respond to external stimuli such as protonation, metal coordination, and oxidation.

Autschbach, Crassous, and co-workers reported pioneering works on the chiroptical switches of bis(pyridine)-containing aza[6]helicenes (Scheme 22).36 2-Pyridyl-aza[6]helicene 47 (Scheme 22a) was synthesized in two steps from 2,2'bipyridine-6-carbaldehyde by the Wittig reaction, followed by a photocyclization reaction.36a The racemate was readily resolved by means of HPLC on a CHIRALPAK IC stationary phase into the enantiomers, which were converted into cycloplatinated derivative 47Pt. Both 47 and 47Pt underwent protonation with HBF₄ to give 47·2H⁺ and 47Pt·H⁺, respectively, which returned with Na₂CO₃ or Et₃N to the neutral forms. Optically active 47 and 47Pt showed CPL and circularly polarized phosphorescence (CPP) with $|g_{lum}|$ values of 3 \times 10⁻³ at around 426 nm and 1×10^{-3} at around 547 nm, respectively. The protonated forms were also CPL and CPP active, and the $|g_{\text{lum}}|$ values of 3 \times 10⁻³ at around 590 nm and 2 \times 10⁻³ at around 555 nm were recorded, respectively. Thus, the acid/base triggered switching of CPL and CPP was achieved. The same group also reported CPL switching systems based on bisaza[6]helicenes 48 and 49 upon Zn2+ binding or protonation (Scheme 22b and c).36b,c

Pieters, Champagne, Audisio, and co-workers synthesized 24 kinds of azahelicenes such as 50 through 1,3-dipolar cycloaddition of sydnones with arynes (Scheme 23).³⁷ Two enantiomers (+)-50 and (-)-50 were successfully separated by HPLC on a CHIRALPAK IC stationary phase. The pyridine-containing azahelicene 50 exhibited high proton affinity, which allowed a chiroptical switch. Whereas (+)-50 showed positive CPL at 430 nm with a g_{lum} of +1.1 \times 10⁻³, (+)-50·H⁺ showed negative CPL at 585 nm with a $g_{\rm lum}$ of -1.2×10^{-3} upon protonation of

Table 1 Chiroptical properties of the representative azahelicenes in this article

Aza[n]helicene		$\Phi_{ m F}$	$ g_{\rm lum} ~(\times~10^{-3})$	$B_{\mathrm{CPL}} \left(\mathrm{M}^{-1} \mathrm{~cm}^{-1} \right)$	$\lambda (nm)^a$	Solvent	Remark	Ref.
1	n = 7	0.39	9	15	473	CH ₂ Cl ₂	$\Phi_{\rm F}$ = 0.80 with TFA	5 <i>a</i>
3	n = 7	0.14	4.4	19	429	$CHCl_3$	$\lambda = 509 \text{ nm with TFA}$	6
4d	n = 7	0.073	3.0	7.4	490	CH_2Cl_2	Solid-state fluorescence	7
6	n = 6	0.21	1.4	1.2	640	CH_3CN	Cationic aza[6]helicene	8 <i>c</i>
7	n = 7	0.08	6.0	14	685	$CHCl_3$	Cationic aza[7]helicene	9
8	n = 6	0.19	28	67	471	$CHCl_3$	Enantioselective synthesis	10 <i>a</i>
11	n = 6	0.059	0.63	<u></u> b	430	CH_2Cl_2	Enantioselective synthesis	11
13	n = 5	0.55	8.5	152	588	CH_2Cl_2	Figure-eight azahelicene dimer	12b
14a	n = 7	0.17	4.2	b	429	2Me-THF	Various derivatives	15
15	n = 7	0.31	1.9	8.8	428	CH_2Cl_2	Various derivatives	16 <i>a</i>
19b	n = 7	0.43	3.5	38	431	toluene	D–A system	18
20a	n = 7	0.34	0.5	4	696	cyclohexane	Radical	19
21	n = 7	0.86	0.22	b	583	CH_2Cl_2	Aromaticity switching	20
22	n = 7	0.99	5.0	100	460	CH_2Cl_2	Azahelicene dimer	21
23	n = 7	0.32	7.0	95	588	CH_2Cl_2	Large racemization barrier	22
24d	_	0.066	21	76	530	CH_2Cl_2	Expanded azahelicene	23 <i>a</i>
25d-Bu	n = 15	0.07	5.7	13	519	THF	Longest CPL-active helicene	24a
26-Bu	n = 9	0.35	1	19	522	THF	Double helicene	24b
27	n = 7	0.45	2.4	173	531	CH_2Cl_2	Double helicene	25
29	n = 5	-b	3	<u></u> b	410	crystal	Crystallization-induced CPL	26
30d	n = 8	0.13	9.5	34	403	CH_2Cl_2	Asymmetric synthesis	27
35	n = 7	0.54	1.3	31	483	CH_2Cl_2	F sensor	28
37	n = 6	0.05	0.98	1	435	CHCl ₃	Enantioselective synthesis	29
38a	n = 7	1	2	28.5	662	CH_2Cl_2	$\Phi_{\rm F}$ = 1 in the red-NIR region, EQE = 28%, TADF	30
39c	n = 7	0.59	2.3	16	485	toluene	$FWHM_{CPL} = 18 \text{ nm}$	31b
40	n = 9	0.98	5.8	220	578	toluene	CP-OLED (EQE = 35.5%, $ g_{EL} = 6.2 \times 10^{-3}$)	31 <i>c</i>
41	n = 6	0.74	2.7	59	598	toluene	Double helicene	31 <i>d</i>
42	n = 9	0.22	3	20	660	toluene	F sensor	31e
44	n = 5	0.65	1	11	522	toluene	F sensor	32
45b	n = 6	0.17	13	59	432	CH_2Cl_2	High g_{lum}	33
46b	n = 10	0.24	48	292	430	CH_2Cl_2	High g_{lum}	34
47	n = 6	0.084	3.4	4.9	426	CH_2Cl_2	CPL switching and CPP	36 <i>a</i>
48	n = 6	0.084	8.6	22	420	CH_2Cl_2	CPL switching and Zn ²⁺ binding	36 <i>b</i>
49	n = 6	0.22	4.8	22	425	CH_2Cl_2	CPL switching and Zn ²⁺ binding	36 <i>c</i>
50	n = 7	0.17	1.1	4	430	CH_2Cl_2	CPL switching	37
52c	n = 7	0.03	1.2	0.8	422	THF	CPL on/off	38
53	n = 7	0.48	0.47	5.8	493	CH_2Cl_2	CPL switching	39

^a Maximum wavelength of fluorescence or CPL. ^b Data not available.

(+)-50 with TFA. Deprotonation was successfully conducted with DBU, and this reversibility enabled at least three-time switches without CPL deterioration. Thus, the pH-triggered chiroptical switch with the distinct color change and signinversion was achieved upon protonation and deprotonation with acid and base, respectively.

Tanaka and co-workers have synthesized heteroatom-doped PAHs via the oxidative fusion reaction of ortho-phenylenebridged cyclic pyrrole/thiophene pentamers. Interestingly, the oxidation of the pentapyrroles with DDQ/Sc(OTf)₃ in toluene at reflux gave pentaaza[10]circulene 51, while that with PIFA in CH₂Cl₂ at -78 °C gave closed-aza[7]helicene 52a (Scheme 24).38a The authors later conducted the oxidation of the substrates containing two or three thiophenes in place of the pyrroles with DDQ/Sc(OTf)3 or FeCl3, which gave the corresponding closed-[7]helicenes 52b and 52c.38b Surprisingly, closed-[7]helicene dimers (52b)₂ and (52c)₂ were obtained when PIFA was used as an oxidant. Furthermore, the closed azahelicenes were found to be interconvertible between the monomers, $52\mathbf{b}$ and $52\mathbf{c}$, and dimers, $(52\mathbf{b})_2$ and $(52\mathbf{c})_2$, via the chemical oxidation and photoreduction. Because only the monomers showed fluorescence and CPL with the $|g_{lum}|$ values

of 4 \times 10⁻⁴ for 52b and 1.2 \times 10⁻³ for 52c, the dimers functioned as light-driven turn-ON CPL emitters.

Maeda, Ema, and co-workers synthesized B,N-embedded πextended helicene 53 (Scheme 25).39 The three-coordinate boron moiety recognized anions to form four-coordinate boron species such as 53·F showing red-shifted and enhanced CPL. The four-coordinate boron species was converted back to 53 with Ag+, and the ion-triggered chiroptical switch was demonstrated.

4. Conclusions

In this feature article, we have summarized recently developed azahelicenes showing CPL. Representative examples are listed in Table 1. A variety of CPL-active azahelicenes have been synthesized by oxidative coupling, cyclization of alkynes or alkenes, photocyclization, and so on. Enantioselective synthesis has also been developed with high ee values reaching >99%. The azahelicenes with imine-type nitrogen undergo protonation or coordination with metal ions, and pH- or coordinationdriven CPL switching systems have been reported. The

azahelicenes with amine-type nitrogen allow facile functionalization such as alkylation, arylation, borylation, and metal complexation, which led to the development of various azahelicene derivatives showing CPL with tunable chiroptical properties. Furthermore, B,N-embedded helicenes have been rapidly growing quite recently because of its potential application as chiral TADF materials and in CP-OLEDs. Some derivatives show fluorescence and CPL in the red-NIR regions with quite high $\Phi_{\rm F}$ values, which leads to high B_{CPL} values and high EQE in the OLEDs. The chiroptical performance has greatly advanced, while it is still difficult to achieve high values of both $\Phi_{\rm F}$ and g_{lum} in the NIR region partly because nonradiative decay often accelerates in the longer wavelength region to decrease $\Phi_{\rm F}$ and because simple π -extension increases the planarity and decreases g_{lum} . Nevertheless, such problems will be solved by combining π -extension, intra- and intermolecular electronic coupling, and molecular recognition systems in the near future. We believe that this feature article will be useful for the further development of new CPL-active helicenes in the future.

Data availability

No primary research results, software or code have been included and no new data were generated or analysed as part of this review.

Conflicts of interest

There are no conflicts to declare.

Acknowledgements

The research on azahelicenes in our group has been supported by JSPS KAKENHI Grant Number 21K05039 and 24K08395.

Notes and references

- 1 (a) H. Maeda and Y. Bando, Pure Appl. Chem., 2013, 85, 1967; (b) E. M. Sánchez-Carnerero, A. R. Agarrabeitia, F. Moreno, B. L. Maroto, G. Muller, M. J. Ortiz and S. de la Moya, Chem. Eur. J., 2015, 21, 13488; (c) J. Kumar, T. Nakashima and T. Kawai, J. Phys. Chem. Lett., 2015, 6, 3445; (d) E. Yashima, N. Ousaka, D. Taura, K. Shimomura, T. Ikai and K. Maeda, Chem. Rev., 2016, 116, 13752; (e) H. Tanaka, Y. Inoue and T. Mori, ChemPhotoChem, 2018, 2, 386; (f) L. Arrico, L. Di Bari and F. Zinna, Chem. - Eur. J., 2021, 27, 2920; (g) K. Takaishi, C. Maeda and T. Ema, Chirality, 2023, 35, 92; (h) C. Maeda, I. Yasutomo, K. Takaishi and T. Ema, J. Porphyrins Phthalocyanines, 2023, 27, 903.
- 2 (a) Y. Shen and C.-F. Chen, Chem. Rev., 2012, 112, 1463; (b) M. Gingras, Chem. Soc. Rev., 2013, 42, 968; (c) M. Gingras, G. Félix and R. Peresutti, Chem. Soc. Rev., 2013, 42, 1007; (d) H. Isla and J. Crassous, C. R. Chimie, 2016, 19, 39; (e) W.-L. Zhao, M. Li, H.-Y. Lu and C.-F. Chen, Chem. Commun., 2019, 55, 13793; (f) K. Dhbaibi, L. Favereau and J. Crassous, Chem. Rev., 2019, 119, 8846; (g) M. Jakubec and J. Storch, J. Org. Chem., 2020, 85, 13415; (h) A. Tsurusaki and K. Kamikawa, Chem. Lett., 2021, **50**, 1913; (i) T. Mori, Chem. Rev., 2021, **121**, 2373; (j) P. Ravat, Chem. – Eur. J., 2021, 27, 3957; (k) M. Cei, L. Di Bari and F. Zinna, Chirality, 2023, 35, 192; (1) A. Nowak-Król, P. T. Geppert and K. R. Naveen, Chem. Sci., 2024, 15, 7408; (m) Q. Huang, Y.-P. Tang, C.-G. Zhang, Z. Wang and L. Dai, ACS Catal., 2024, 14, 16256.

- 3 (a) Y. Nakai, T. Mori and Y. Inoue, J. Phys. Chem. A, 2013, 117, 83; (b) S. Abbate, G. Longhi, F. Lebon, E. Castiglioni, S. Superchi, L. Pisani, F. Fontana, F. Torricelli, T. Caronna, C. Villani, R. Sabia, M. Tommasini, A. Lucotti, D. Mendola, A. Mele and D. A. Lightner, J. Phys. Chem. C, 2014, 118, 1682.
- 4 (a) P. G. Campbell, A. J. V. Marwitz and S.-Y. Liu, Angew. Chem., Int. Ed., 2012, 51, 6074; (b) Z. X. Giustra and S.-Y. Liu, J. Am. Chem. Soc., 2018, 140, 1184; (c) X. Chen, D. Tan and D.-T. Yang, J. Mater. Chem. C, 2022, 10, 13499; (d) C. Chen, Y. Zhang, X.-Y. Wang, J.-Y. Wang and J. Pei, Chem. Mater., 2023, 35, 10277; (e) M. Mamada, M. Hayakawa, J. Ochi and T. Hatakeyama, Chem. Soc. Rev., 2024, 53, 1624.
- 5 (a) T. Otani, A. Tsuyuki, T. Iwachi, S. Someya, K. Tateno, H. Kawai, T. Saito, K. S. Kanyiva and T. Shibata, Angew. Chem., Int. Ed., 2017, 56, 3906; (b) T. Otani, T. Sasayama, C. Iwashimizu, K. S. Kanyiva, H. Kawai and T. Shibata, Chem. Commun., 2020, 56, 4484.
- 6 T. Taniguchi, Y. Nishii, T. Mori, K. Nakayama and M. Miura, Chem. -Eur. J., 2021, 27, 7356.
- 7 J. Feng, L. Wang, X. Xue, Z. Chao, B. Hong and Z. Gu, Org. Lett., 2021, 23, 8056.
- 8 (a) I. Hernández Delgado, S. Pascal, A. Wallabregue, R. Duwald, C. Besnard, L. Guénée, C. Nançoz, E. Vauthey, R. C. Tovar, J. L. Lunkley, G. Muller and J. Lacour, Chem. Sci., 2016, 7, 4685; (b) S. Pascal, C. Besnard, F. Zinna, L. Di Bari, B. Le Guennic, D. Jacquemin and J. Lacour, Org. Biomol. Chem., 2016, 14, 4590; (c) R. Duwald, J. Bosson, S. Pascal, S. Grass, F. Zinna, C. Besnard, L. Di Bari, D. Jacquemin and J. Lacour, Chem. Sci., 2020, 11, 1165; (d) P. Moneva Lorente, A. Wallabregue, F. Zinna, C. Besnard, L. Di Bari and J. Lacour, Org. Biomol. Chem., 2020, 18, 7677.
- 9 C. Olivier, N. Nagatomo, T. Mori, N. McClenaghan, G. Jonusauskas, B. Kauffmann, Y. Kuwahara, M. Takafuji, H. Ihara and Y. Ferrand, Org. Chem. Front., 2023, 10, 752.
- 10 (a) K. Nakamura, S. Furumi, M. Takeuchi, T. Shibuya and K. Tanaka, J. Am. Chem. Soc., 2014, 136, 5555; (b) K. Hanada, J. Nogami, K. Miyamoto, N. Hayase, Y. Nagashima, Y. Tanaka, A. Muranaka, M. Uchiyama and K. Tanaka, Chem. - Eur. J., 2021, 27, 9313.
- 11 T. Yu, Z.-Q. Li, J. Li, S. Cheng, J. Xu, J. Huang, Y.-W. Zhong, S. Luo and Q. Zhu, ACS Catal., 2022, 12, 13034.
- 12 (a) K. Goto, R. Yamaguchi, S. Hiroto, H. Ueno, T. Kawai and H. Shinokubo, Angew. Chem., Int. Ed., 2012, 51, 10333; (b) A. Ushiyama, S. Hiroto, J. Yuasa, T. Kawai and H. Shinokubo, Org. Chem. Front., 2017, 4, 664.
- 13 (a) G. M. Upadhyay, H. R. Talele, S. Sahoo and A. V. Bedekar, Tetrahedron Lett., 2014, 55, 5394; (b) G. M. Upadhyay and A. V. Bedekar, Tetrahedron, 2015, 71, 5644; (c) G. M. Upadhyay, H. R. Talele and A. V. Bedekar, J. Org. Chem., 2016, 81, 7751; (d) C. Maeda, K. Akiyama and T. Ema, Org. Lett., 2023, 25, 3932.
- 14 (a) K. Nakano, Y. Hidehira, K. Takahashi, T. Hiyama and K. Nozaki, Angew. Chem., Int. Ed., 2005, 44, 7136; (b) K. Uematsu, K. Noguchi and K. Nakano, Phys. Chem. Chem. Phys., 2018, 20, 3286; (c) X.-Y. Chen, J.-K. Li, C. Wang and X.-Y. Wang, Tetrahedron Lett., 2024, 139, 154981.
- 15 K. Uematsu, C. Hayasaka, K. Takase, K. Noguchi and K. Nakano, Molecules, 2022, 27, 606.
- 16 (a) C. Maeda, K. Nagahata, T. Shirakawa and T. Ema, Angew. Chem., Int. Ed., 2020, 59, 7813; (b) C. Maeda, S. Nomoto, K. Akiyama, T. Tanaka and T. Ema, Chem. – Eur. J., 2021, 27, 15699; (c) C. Maeda, S. Michishita and T. Ema, Chem. - Eur. J., 2025, 31, e202404325.
- 17 (a) C. Maeda, K. Nagahata, K. Takaishi and T. Ema, Chem. Commun., 2019, 55, 3136; (b) C. Maeda, K. Suka, K. Nagahata, K. Takaishi and T. Ema, Chem. – Eur. J., 2020, 26, 4261; (c) C. Maeda, S. Nomoto, K. Takaishi and T. Ema, Chem. - Eur. J., 2020, 26, 13016.
- 18 X.-Y. Chen, J.-K. Li, W.-L. Zhao, C.-Z. Du, M. Li, C.-F. Chen and X.-Y. Wang, J. Mater. Chem. C, 2023, 11, 893.
- 19 M. Gross, F. Zhang, M. E. Arnold, P. Ravat and A. J. C. Kuehne, Adv. Opt. Mater., 2024, 12, 2301707.
- 20 C. Li, C. Zhang, P. Li, Y. Jia, J. Duan, M. Liu, N. Zhang and P. Chen, Angew. Chem., Int. Ed., 2023, 62, e202302019.
- 21 Y. Shi, C. Li, J. Di, Y. Xue, Y. Jia, J. Duan, X. Hu, Y. Tian, Y. Li, C. Sun, N. Zhang, Y. Xiong, T. Jin and P. Chen, Angew. Chem., Int. Ed., 2024, 63, e202402800.
- 22 S. Qiu, A. C. Valdivia, W. Zhuang, F.-F. Hung, C.-M. Che, J. Casado and J. Liu, J. Am. Chem. Soc., 2024, 146, 16161.
- 23 (a) G.-F. Huo, W.-T. Xu, Y. Han, J. Zhu, X. Hou, W. Fan, Y. Ni, S. Wu, H.-B. Yang and J. Wu, Angew. Chem., Int. Ed., 2024, 63, e202403149;

- (b) G.-F. Huo, T. M. Fukunaga, X. Hou, Y. Han, W. Fan, S. Wu, H. Isobe and J. Wu, Angew. Chem., Int. Ed., 2023, 62, e202218090.
- 24 (a) Y. Matsuo, M. Gon, K. Tanaka, S. Seki and T. Tanaka, J. Am. Chem. Soc., 2024, 146, 17428; (b) Y. Matsuo, M. Gon, K. Tanaka, S. Seki and T. Tanaka, Chem. - Asian J., 2024, 19, e202400134.
- 25 J. Liu, J. Hong, Z. Liao, J. Tan, H. Liu, E. Dmitrieva, L. Zhou, J. Ren, X.-Y. Cao, A. A. Popov, Y. Zou, A. Narita and Y. Hu, Angew. Chem., Int. Ed., 2024, 63, e202400172.
- 26 P. Jiang, A. S. Mikherdov, H. Ito and M. Jin, J. Am. Chem. Soc., 2024, 146, 12463.
- T. Yanagi, T. Tanaka and H. Yorimitsu, Chem. Sci., 2021, 12, 2784.
- C. Maeda, I. Yasutomo and T. Ema, Angew. Chem., Int. Ed., 2024, 63, e202404149.
- W.-L. Xu, R.-X. Zhang, H. Wang, J. Chen and L. Zhou, Angew. Chem., Int. Ed., 2024, 63, e202318021.
- (a) Y. Zhang, D. Zhang, T. Huang, A. J. Gillett, Y. Liu, D. Hu, L. Cui, Z. Bin, G. Li, J. Wei and L. Duan, Angew. Chem., Int. Ed., 2021, 60, 20498; (b) J.-K. Li, X.-Y. Chen, Y.-L. Guo, X.-C. Wang, A. C.-H. Sue, X.-Y. Cao and X.-Y. Wang, J. Am. Chem. Soc., 2021, 143, 17958.
- 31 (a) F. Zhang, F. Rauch, A. Swain, T. B. Marder and P. Ravat, Angew. Chem., Int. Ed., 2023, 62, e202218965; (b) F. Zhang, V. Brancaccio, F. Saal, U. Deori, K. Radacki, H. Braunschweig, P. Rajamalli and P. Ravat, J. Am. Chem. Soc., 2024, 146, 29782; (c) W.-C. Guo, W.-L. Zhao, K.-K. Tan, M. Li and C.-F. Chen, Angew. Chem., Int. Ed., 2024, 63, e202401835; (d) Y.-Y. Ju, L.-E. Xie, J.-F. Xing, Q.-S. Deng, X.-W. Chen, L.-X. Huang, G.-H. Nie, Y.-Z. Tan and B. Zhang, Angew. Chem., Int. Ed., 2024, 63, e202414383; (e) W. Zhuang, F.-F. Hung, C.-M. Che and J. Liu, Angew. Chem., Int. Ed., 2024, 63, e202406497.
- 32 D. Tan, J. Dong, T. Ma, Q. Feng, S. Wang and D.-T. Yang, Angew. Chem., Int. Ed., 2023, 62, e202304711.
- 33 Y. Appiarius, S. Míguez-Lago, P. Puylaert, N. Wolf, S. Kumar, M. Molkenthin, D. Miguel, T. Neudecker, M. Juríček, A. G. Campaña and A. Staubitz, Chem. Sci., 2024, 15, 466.
- 34 Y. Yu, C. Wang, F.-F. Hung, C. Chen, D. Pan, C.-M. Che and J. Liu, J. Am. Chem. Soc., 2024, 146, 22600.

- 35 (a) H. Maeda, Y. Bando, K. Shimomura, I. Yamada, M. Naito, H. Nobusawa, H. Tsumatori and T. Kawai, J. Am. Chem. Soc., 2011, 133, 9266; (b) B. A. San Jose, J. Yan and K. Akagi, Angew. Chem., Int. Ed., 2014, 53, 10641; (c) Y. Nagata, T. Nishikawa and M. Suginome, Chem. Commun., 2014, 50, 9951; (d) S. P. Morcillo, D. Miguel, L. A. de Cienfuegos, J. Justicia, S. Abbate, E. Castiglioni, C. Bour, M. Ribagorda, D. J. Cárdenas, J. M. Paredes, L. Crovetto, D. Choquesillo-Lazarte, A. J. Mota, M. C. Carreño, G. Longhi and J. M. Cuerva, Chem. Sci., 2016, 7, 5663; (e) Y. Hashimoto, T. Nakashima, D. Shimizu and T. Kawai, Chem. Commun., 2016, 52, 5171; (f) S. Ito, K. Ikeda, S. Nakanishi, Y. Imai and M. Asami, Chem. Commun., 2017, 53, 6323; (g) K. Takaishi, M. Yasui and T. Ema, J. Am. Chem. Soc., 2018, 140, 5334; (h) A. Homberg, E. Brun, F. Zinna, S. Pascal, M. Górecki, L. Monnier, C. Besnard, G. Pescitelli, L. Di Bari and J. Lacour, Chem. Sci., 2018, 9, 7043; (i) S. Fa, T. Tomita, K. Wada, K. Yasuhara, S. Ohtani, K. Kato, M. Gon, K. Tanaka, T. Kakuta, T. Yamagishi and T. Ogoshi, Chem. Sci., 2022, 13, 5846; (j) Y. Wang, J. Gong, X. Wang, W.-J. Li, X.-Q. Wang, X. He, W. Wang and H.-B. Yang, Angew. Chem., Int. Ed., 2022, **61**, e202210542.
- 36 (a) N. Saleh, B. Moore, M. Srebro, N. Vanthuyne, L. Toupet, J. A. G. Williams, C. Roussel, K. K. Deol, G. Muller, J. Autschbach and J. Crassous, Chem. - Eur. J., 2015, 21, 1673; (b) H. Isla, M. Srebro-Hooper, M. Jean, N. Vanthuyne, T. Roisnel, J. L. Lunkley, G. Muller, J. A. G. Williams, J. Autschbach and J. Crassous, Chem. Commun., 2016, **52**, 5932; (c) H. Isla, N. Saleh, J.-K. Ou-Yang, K. Dhbaibi, M. Jean, M. Dziurka, L. Favereau, N. Vanthuyne, L. Toupet, B. Jamoussi, M. Srebro-Hooper and J. Crassous, J. Org. Chem., 2019, 84, 5383.
- 37 E. Yen-Pon, F. Buttard, L. Frédéric, P. Thuéry, F. Taran, G. Pieters, P. A. Champagne and D. Audisio, JACS Au, 2021, 1, 807.
- 38 (a) Y. Matsuo, K. Kise, Y. Morimoto, A. Osuka and T. Tanaka, Angew. Chem., Int. Ed., 2022, 61, e202116789; (b) Y. Matsuo, C. Maeda, Y. Tsutsui, T. Tanaka and S. Seki, Angew. Chem., Int. Ed., 2023, 62, e202314968.
- 39 C. Maeda, S. Michishita, I. Yasutomo and T. Ema, Angew. Chem., Int. Ed., 2025, 64, e202418546.